Co-doped amorphous $NiMoS_4$ modified with rGO for high-rate and long-cycle stability of hybrid supercapacitor

Yuchen Lu,[a] Bingji Huang,[a] Jingjing Yuan*[a], Yifan Qiao,[a] Wenyao Zhang,[b] Guangyu He,[a] Haiqun Chen*[a]

([a]Jiangsu Key Laboratory of Advanced Catalytic Materials and Technology, Advanced Catalysis and Green Manufacturing Collaborative Innovation Centre, Changzhou University, Changzhou, Jiangsu Province 213164, China;

[b]Key Laboratory for Soft Chemistry and Functional Materials of Ministry of Education, Nanjing University of Science and Technology, Nanjing, 210094, China)

*Jingjing Yuan. E-mail: yuanjj@cczu.edu.cn *Haiqun Chen. E-mail: chenhq@cczu.edu.cn

1. Experimental section

1.1 Materials

$(NH_4)_2S$ solution (16~20%), $NH_3 \cdot H_2O$ (30~33%), $(NH_4)_6Mo_7O_{24} \cdot 4H_2O$, $Ni(NO_3)_2 \cdot 6H_2O$, $Co(NO_3)_2 \cdot 6H_2O$, concentrated H_2SO_4 (95~98%), $KMnO_4$, KOH and polytetrafluoroethylene (PTFE) were purchased from Sinopharm Chemical Reagent Co., Ltd (China). Needle Coke (carbon content ≥ 98% and ash content ≤ 0.8%) was purchased from Jinzhou Petrochemical Co., Ltd (China). All reagents and solvents were of analytical grade and used as received.

1.2 Preparation of GO

Graphite oxide (GO) is prepared by a modified Hummers method.

1.3 Preparation of $(NH_4)_2MoS_4$

The preparation method of $(NH_4)_2MoS_4$ has been improved on the basis of the work of our group[1]. 19.6 g of $(NH_4)_6Mo_7O_{24} \cdot 4H_2O$ were dissolved in 50 mL of ammonia water, and the pH of the ammonia water was adjusted to 9 using $NH_3 \cdot H_2O$. The solution was stirred in a water bath at 65 °C for 1 h after

340 mL of $(NH_4)_2S$ solution was added. Following this, the solution was crystallized in an ice-water bath at 0 °C for 1 h. The resulting material was washed with deionized water and vacuum-dried for 12 h at 60 °C to give $(NH_4)_2MoS_4$.

1.4 Preparation of $Ni_{1-x}Co_xMoS_4$/rGO composite

The preparation process taking $Ni_{0.7}Co_{0.3}MoS_4$/rGO as an example is as follows: 0.13 g of $(NH_4)_2MoS_4$ was dissolved in 20 mL of deionized water in a 60 °C water bath. At the same time, 0.102 g of $Ni(NO_3)_2·6H_2O$ and 0.044 g of $Co(NO_3)_2·6H_2O$ were added to 40 mL of GO dispersion with 16 mg dispersed in it, stirred at a constant speed for 10 min, and then sonicated for 20 min. Then the cooled $(NH_4)_2MoS_4$ solution was slowly added dropwise to the above dispersion, stirred at a constant speed for 30 min, and reacted at 120 °C for 12 h. The samples were centrifuged three times with deionized water and then freeze-dried to obtain a black powder sample. A series of $Ni_{1-x}Co_xMoS_4$/rGO (x=0, 0.3, 0.5, 0.7 and 1) composites were prepared by adjusting the molar ratio of nickel-cobalt metal salts. For comparison, $NiMoS_4$ and $Ni_{0.7}Co_{0.3}MoS_4$ were prepared under the same conditions without adding GO.

1.5 Preparation of needle coke oxide (NCO)

1 g of the needle coke (NC) was slowly added to a beaker containing 25 mL of concentrated H_2SO_4 under ice-water bath, and stirred for 1 h. Then 3 g of $KMnO_4$ was slowly added in an ice-water bath and kept stirring for 12 h at room temperature. After that, 60 mL of deionized water was slowly added to the above mixture, stirring for 12 h at 60 °C. Finally, the product was rinsed to neutrality with deionized water and dried at 60 °C in oven, named as NCO.

1.6 Materials characterization

The crystalline phase was investigated by powder X-ray diffraction (XRD, Bruker D8 Advance with Cu Kα radiation, λ = 0.15418 nm). The specific surface area was obtained from the N_2 adsorption-

desorption isotherms and calculated by the Brunauer-Emmett-Teller method (BET, ASAP2460). The chemical species and structure of samples were examined by X-ray photoelectron spectroscopy (XPS, Thermo Scientific K-Alpha) and Fourier transform infrared spectroscopy (FT-IR, Nicolet Avatar 370). The morphology of samples was observed by field-emission scanning electron microscopy (FESEM, Zeiss Supra 55) equipped with an energy dispersive spectrometer (EDS) and transmission electron microscopy (TEM, JEOL JEM-2100).

1.7 Electrochemical measurements

Electrochemical studies were conducted using three-electrode and two-electrode systems. Acetylene black and polytetrafluoroethylene (PTFE) were used as the conductive component and binder, respectively. The active material, acetylene black, and PTFE were uniformly mixed in an 8:1:1 mass ratio, and the resulting slurry was uniformly coated on a porous NF substrate with a 1 cm×1 cm area. The mass of the active ingredient is approximately 1.2 mg. As the electrolyte, a KOH solution of 6 mol L^{-1} was used. The platinum rod and the Hg/HgO electrode serve as the counter and reference electrodes in the three-electrode test, respectively. For the two-electrode test, a CR2032 battery box was used, and glass fiber filter paper was used as a separator to construct a two-electrode symmetrical button capacitor. The cyclic voltammetry (CV) and galvanostatic charge-discharge (GCD) tests of the samples were performed using the CHI 760E electrochemical workstation of Shanghai Chenhua Company. All electrochemical tests were performed at room temperature.

The specific capacitance C ($C \cdot g^{-1}$) of the three-electrode system was calculated using the equation[2]:

$$C = \frac{I\Delta t}{m} \quad (1)$$

where m is the weight of the active material, Δt is the discharge duration, I is the discharge current.

The following equations are used to compute the power density P ($W \cdot kg^{-1}$) and energy density E ($Wh \cdot kg^{-1}$) of the HSC[3]:

$$E = \frac{C\Delta V}{7.2} \quad (2)$$

$$P = \frac{3600E}{\Delta t} \quad (3)$$

where C represents the specific capacitance of the HSC ($C \cdot g^{-1}$), and ΔV and Δt are equivalent to those in equations (1).

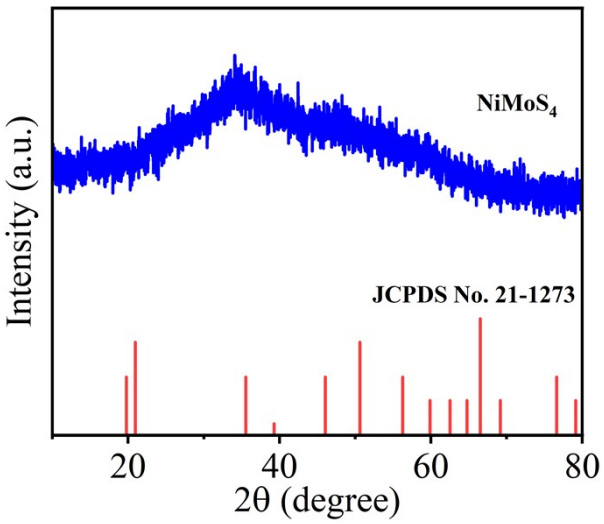

Fig. S1 XRD spectra of $NiMoS_4$ and standard card

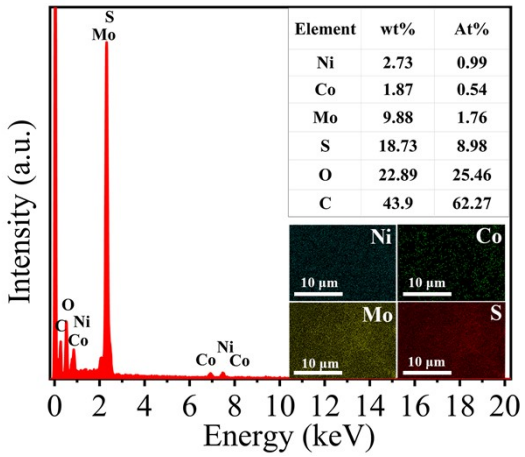

Fig. S2 The EDS spectra of $Ni_{0.7}Co_{0.3}MoS_4$/rGO (the inset shows the Ni, Co, Mo and S elemental mappings).

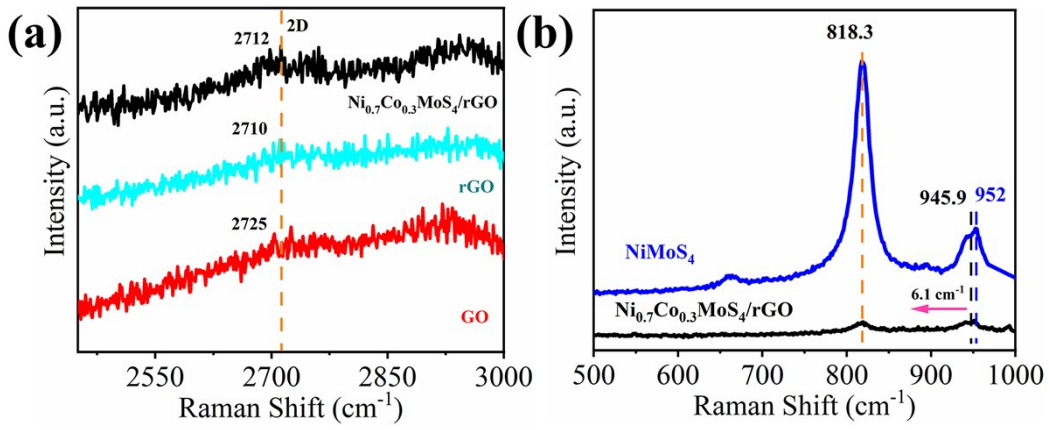

Fig. S3 (a) Amplified Raman spectra of GO, RGO and $Ni_{0.7}Co_{0.3}MoS_4$/rGO from 2450 cm^{-1} to 3000 cm^{-1}, (b) Amplified Raman spectra of $NiMoS_4$ and $Ni_{0.7}Co_{0.3}MoS_4$/rGO from 500 cm^{-1} to 1000 cm^{-1}

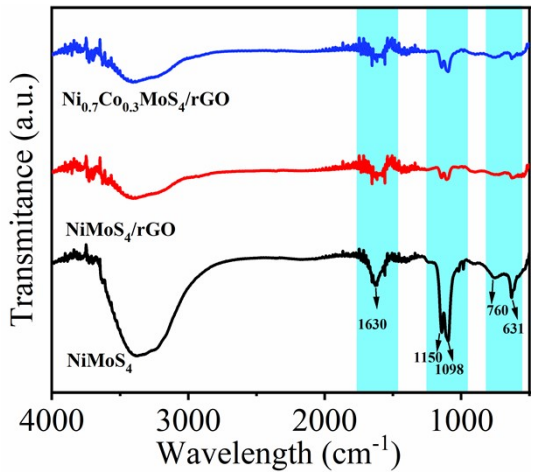

Fig. S4 FT-IR spectra of $NiMoS_4$, $NiMoS_4$/rGO and $Ni_{0.7}Co_{0.3}MoS_4$/rGO

Fig. S4 clearly shows that rGO has weak absorption bands at 1630, 1403, 1150 and 1098 cm^{-1}, which is caused by functional groups such as -OH, -O and -OOH on the surface.[4] In addition, the tensile vibration peaks of Ni-S and Mo-S appeared at 760 and 631 cm^{-1} respectively.[5] With the introduction of Co, the Ni-S and Mo-S peak intensities of the $Ni_{0.7}Co_{0.3}MoS_4$/rGO curve are also weakened. These results indicate that $NiMoS_4$ and $Ni_{0.7}Co_{0.3}MoS_4$/rGO were successfully prepared.

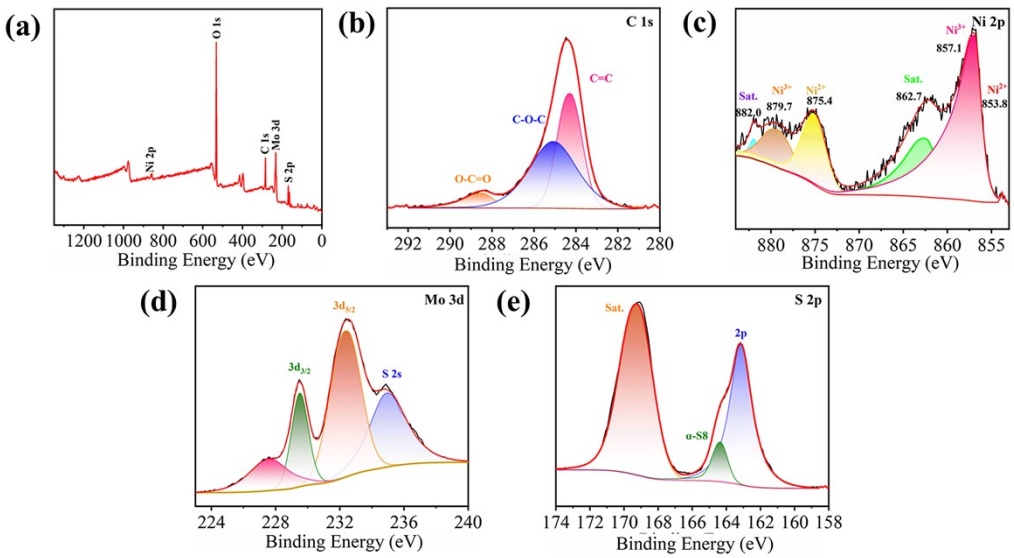

Fig. S5 (a) XPS survey spectrum of $NiMoS_4$/rGO. Core XPS spectrum of (b) C 1s, (c) Ni 2p, (d) Mo 3d and (e) S 2p XPS spectra of $NiMoS_4$/rGO

The Ni 2p spectrum of $NiCoMoS_4$/rGO can be fitted into the satellite peaks (862.7 and 882.0 eV), corresponding to Ni^{3+} (879.7 and 857.1 eV) and Ni^{2+} (875.4 and 853.8 eV) characteristic peaks. The above data can prove that compared with $NiMoS_4$/rGO, the Ni characteristic peaks of $Ni_{0.7}Co_{0.3}MoS_4$/rGO generally have obvious red shift.

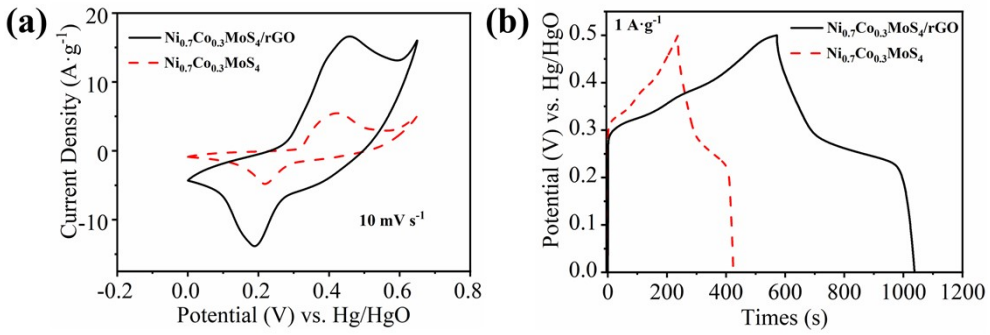

Fig. S6 CV (a) and GCD (b) curves of $Ni_{0.7}Co_{0.3}MoS_4$ and $Ni_{0.7}Co_{0.3}MoS_4$/rGO.

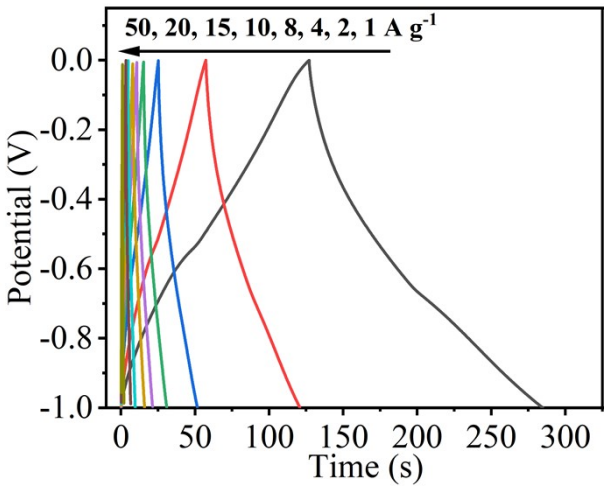

Fig. S7 GCD curves of NCO in different current density.

Table S1 Comparison of electrochemical performance of $Ni_{0.7}Co_{0.3}MoS_4$/rGO (three-electrode system) with reported transition metal-based sulfides electrode in literatures

Electrode material	Specific capacity	References
$Ni_{0.7}Co_{0.3}MoS_4$/rGO	**509.8 C·g^{-1} at 1 A·g^{-1}**	**This work**
Amorphous $CoMoS_4$	396.6 C·g^{-1} at 1 A·g^{-1}	6
Amorphous structured $NiMoS_4$-rGO	500 C·g^{-1} at 1 A·g^{-1}	7
$NiCo_2S_4$ nanotube	397 C·g^{-1} at 1 A·g^{-1}	8
$NiCo_2O_4$ flowerlike nanostructure	361.9 C·g^{-1} at 1 A·g^{-1}	9
$NiCo_2S_4$@MnO_2 heterostructure	286.4 C·g^{-1} at 1 A·g^{-1}	10
$NiCo_2S_4$ cubic octahedron	334 C·g^{-1} at 1 A·g^{-1}	11
rGO_{100}-CNT_{50}-Co_3S_4	488.6 C·g^{-1} at 1 A·g^{-1}	12
Ni_3S_4-MoS_2 nano flower	490.8 C·g^{-1} at 1 A·g^{-1}	13
MOF-derived Co_9S_8/carbon	367 C·g^{-1} at 1 A·g^{-1}	14
Co_3O_4-rGO	330 C·g^{-1} at 0.5 A·g^{-1}	15

Table S2 Rate performance of $NiMoS_4$/rGO, $Ni_{0.7}Co_{0.3}MoS_4$/rGO, $Ni_{0.5}Co_{0.5}MoS_4$/rGO, $Ni_{0.3}Co_{0.7}MoS_4$/rGO and $CoMoS_4$/rGO

Electrode material	Capacitance in 1 $A \cdot g^{-1}$ ($C \cdot g^{-1}$)	Capacitance in 20 $A \cdot g^{-1}$($C \cdot g^{-1}$)	Capacitance retention (%)
$NiMoS_4$/rGO	114.1	36	31
$Ni_{0.7}Co_{0.3}MoS_4$/rGO	509.8	260.3	51
$Ni_{0.5}Co_{0.5}MoS_4$/rGO	312	76.8	24.6
$Ni_{0.3}Co_{0.7}MoS_4$/rGO	140	34.6	24.7
$CoMoS_4$/rGO	370	23.8	6.4

Reference

1. B. Huang, J. Yuan, Y. Lu, Y. Zhao, X. Qian, H. Xu, G. He and H. Chen, *Chem. Eng. J.*, 2022, 436.

2. B. Huang, D. Yao, J. Yuan, Y. Tao, Y. Yin, G. He and H. Chen, *J. Colloid Interface Sci.*, 2022, 606, 1652-1661.

3. H. Peng, B. Yao, X. Wei, T. Liu, T. Kou, P. Xiao, Y. Zhang and Y. Li, *Advanced Energy Materials*, 2019, 9.

4. X. Zhao, M. Chen, H. Wang, L. Xia, M. Guo, S. Jiang, Q. Wang, X. Li and X. Yang, *Mater Sci Eng C Mater Biol Appl*, 2020, 116, 111221.

5. J. Xu, X. Yang, Y. Zou, L. Zhu, F. Xu, L. Sun, C. Xiang and J. Zhang, *J. Alloys Compd.*, 2022, 891.

6. X. Xu, Y. Song, R. Xue, J. Zhou, J. Gao and F. Xing, *Chem. Eng. J.*, 2016, 301, 266-275.

7. M. Wei, X. Wu, Y. Yao, S. Yu, R. Sun and C. Wong, *ACS Sustainable Chemistry & Engineering*, 2019, 7, 19779-19786.

8. H. Wang, M. Liang, Z. He, Z. Guo, Y. Zhao, K. Li, W. Song, Y. Zhang, X. Zhang, Y. Zhao and Z. Miao, *Current Applied Physics*, 2022, 35, 7-15.

9. H. Chen, J. Jiang, L. Zhang, T. Qi, D. Xia and H. Wan, *J. Power Sources*, 2014, 248, 28-36.

10. H. Chen, X. L. Liu, J. M. Zhang, F. Dong and Y. X. Zhang, *Ceram. Int.*, 2016, 42, 8909-8914.

11. S. Hussain, T. Liu, N. Aslam, Y. Zhang and S. Zhao, *Mater. Lett.*, 2017, 189, 21-24.

12. A. Mohammadi, N. Arsalani, A. G. Tabrizi, S. E. Moosavifard, Z. Naqshbandi and L. S. Ghadimi, *Chem. Eng. J.*, 2018, 334, 66-80.

13. W. Luo, G. Zhang, Y. Cui, Y. Sun, Q. Qin, J. Zhang and W. Zheng, *Journal of Materials Chemistry A*, 2017, 5, 11278-11285.

14. S. Zhang, D. Li, S. Chen, X. Yang, X. Zhao, Q. Zhao, S. Komarneni and D. Yang, *Journal of Materials Chemistry A*, 2017, 5, 12453-12461.

15. L. Xie, F. Su, L. Xie, X. Li, Z. Liu, Q. Kong, X. Guo, Y. Zhang, L. Wan, K. Li, C. Lv and C. Chen, *ChemSusChem*, 2015, 8, 2917-2926.